Complex loss function of CdTe

H. Dröge
Physikalisches Institut, Universität Würzburg, Am Hubland, D-97074 Würzburg, Germany

A. Fleszar and W. Hanke
Institut für Theoretische Physik, Universität Würzburg, Am Hubland, D-97074 Würzburg, Germany

M. Sing, M. Knupfer, and J. Fink
Institut für Festkörper- und Werkstofforschung Dresden, Postfach 270016, D-01171 Dresden, Germany

F. Goschenhofer, C. R. Becker, R. Kargerbauer, and H. P. Steinrück
Physikalisches Institut, Universität Würzburg, Am Hubland, D-97074 Würzburg, Germany

(Received 16 September 1998)

We report results of high-resolution electron energy-loss measurements in transmission of CdTe films. In contrast to simple metals and other semiconductors studied experimentally so far, our results show a number of loss structures of comparable strength occupying a rather narrow energy region around the classical plasmon energy. With increasing momentum transfer these structures show no or only weak dispersion and the relative spectral weight shifts from the energetically lowest to the highest feature. The measurements are analyzed using *ab initio* calculations of the CdTe loss function. [S0163-1829(99)07407-X]

I. INTRODUCTION

One of the basic features of extended systems of charged particles is their ability to be excited in the form of plasmons—collective oscillation waves of electrons against the rigid ''background'' of positively charged ionic cores.[1] The very existence of plasmons is a classical phenomenon and for many materials the plasmon energy is given with a good approximation by the mean electron density n through the classical relation[2] $E_p=(4\pi ne^2/m)^{1/2}$. Solid-state effects are, however, usually not negligible and influence the energy of plasmons, their dispersion and width via the band structure of materials or via many-body interactions.[3] In materials of a more complicated band structure, especially where an interplay between localized and delocalized electrons is important, interaction effects can lead to qualitatively new situations as compared to the classical picture. A good example is the case of silver, where apart from the classical, free-electron plasmon at 8 eV, an additional very sharp plasmon at 3.8 eV appears.[1]

In this paper, we report about another manifestation of solid-state effects, namely, the occurrence of a *complex of loss structures* of comparable strengths instead of one single, damped plasmon. In high-resolution electron energy-loss spectroscopy (EELS) transmission experiments[1] on CdTe single crystals we observe a group of three main and a few less pronounced peaks of energies between 11.9 and 16.3 eV. Using *ab initio* calculations of the bulk dielectric function and the loss function of CdTe, we analyze the experimental spectra and show that the multipeak structure originates from the presence of two interband transitions from the occupied Cd $4d$ states into high-density regions of unoccupied states. Since the energy of these interband transitions is very close to the energy of the ''free-electron'' plasmon in CdTe, a strong interference of both effects takes place, which results in a complex structure of the loss function. A similar behavior is expected in other II-VI compounds with a shallow semicore states.

Our experiments are, to our knowledge, the first EELS investigations of a material from the class II-VI done with high resolution.[4] We have performed our measurements with a primary electron energy of 170 keV and various momentum transfers ranging between 0.07 and 0.83 Å^{-1} in the [111] and [110] crystallographic directions. Previous studies have been performed mainly by reflection electron energy-loss spectroscopy (REELS) on CdTe[110] (Refs. 5–8) and CdTe[100].[9] In addition, there are also transmission EELS studies without q resolution,[8,10,11] performed, however, with much smaller primary electron energy than in our investigation and an electron-beam cross-sectional analysis.[12] The advantage of EELS measurements in transmission lies in the enhancement of the probability of bulk losses as compared to REELS, which is strongly surface sensitive. Furthermore, the EELS experiments are performed with a much bigger primary electron energy, which better satisfies the validity of the first Born approximation. This is necessary in order to relate the experimental results to the response functions of the (unperturbed) system, i.e., to its two-particle excitation spectrum. Experimental access to this spectrum at $q=0$ Å^{-1} can be achieved also by other methods, e.g., by optical measurements, which are well established due to their high precision. CdTe has also been studied by optical means: reflectivity,[13] ellipsometry,[14,15] optical absorption,[16] and by the extended synchrotron x-ray reflectivity.[17]

On the theoretical side, there is a very recent *ab initio* calculation of the bulk loss properties of a series of Cd-based II-VI compounds for momentum transfers along the (100) direction.[18] According to this calculation, there appears a number of loss structures in these materials and the dominant loss peak in all II^B-VI compounds theoretically studied shows a rather unusual, negative dispersion with growing momentum transfer q. It was also found that the loss function of CdTe is sensitive to various computational factors, such as the presence and the correct energy position of semicore Cd $4d$ states, or the many-body corrections in screening. There-

fore, a comparison of our EELS measurements with theoretical predictions should not only test the accuracy of the latter, but also bring an experimental verification of the various computational ingredients. In order to enable such an accurate comparison, we have performed detailed calculations, computationally similar to those in Ref. 18.

In the next sections we present the experimental setup, some computational details and discuss the results. The origin of the multiplasmon shape of the loss spectrum will be analyzed in detail.

II. EXPERIMENT

The transmission EELS measurements were performed using a dedicated spectrometer at the Institut für Festkörper- und Werkstofforschung (IFW) in Dresden, Germany. It was operated with a primary energy of 170 keV and the energy and momentum resolution were 120 meV and 0.05 Å^{-1}, respectively (for details see Ref. 4). Due to the finite mean-free path of electrons, only samples up to a thickness of about 100 nm can be investigated at the primary energy used in our experiment.

The CdTe samples were prepared using a new preparation procedure; a detailed description of the method and the sample characterization by means of TEM (transmission electron microscope) and x-ray diffraction will be given elsewhere.[19] Briefly, a CdTe film of 100 nm thickness was grown on a GaAs(100) substrate at 260 °C in the central molecular-beam epitaxy facility at the University of Würzburg. Under these conditions one obtains epitaxial CdTe(100) layers (despite the large lattice mismatch of CdTe and GaAs of $\sim$14%) that are completely relaxed after a few monolayers have been deposited. X-ray diffraction shows that the CdTe films are of high structural quality and that the growth direction deviates from the nominal [100] direction by about 0.12°.[19]

After the growth process the sample was exposed to air and was mechanically polished on the substrate side down to a thickness of about 100 μm. Thereafter, the remaining GaAs substrate was chemically removed by a very dilute mixture of H_2O_2 and NaOH leaving a free-standing, clean CdTe film of about 100 nm thickness. This film was then attached to a standard TEM copper mesh, which is used as sample holder.

III. THEORETICAL CONSIDERATIONS

The experimental results are compared with the calculated *loss functions* for various momentum transfers $\vec{q}$ in the [111] direction. The computational scheme was analogous to that used in Ref. 18. The starting point of our calculations consisted of a band structure, which has been obtained within the local-density approximation (LDA) using a mixed basis code (localized, *d*-type gaussians centered at the Cd sites and plane waves with a cutoff of 12.5 Ry). Electron-ion interaction has been modeled by a nonlocal pseudopotential taking explicitly into account the Cd $4d$ states as valence states.[20] The LDA exchange-correlation energy functional has been taken as in Ref. 21. Since the LDA approximation[22] severely underestimates the binding energy of the localized semicore Cd $4d$ states, we have constructed an empirical correction to the *d* component of the Cd^{12+} pseudopotential in such a way, that the resulting position of Cd $4d$ bands agrees with the measured position of these states in photoemission experiments. It was shown in Ref. 18 that such a correction (which empirically models many-body effects on the localized Cd $4d$ states) leads to a significant change of the shape of the loss function in CdTe. In Fig. 1 the resulting band structure, including spin-orbit interaction, is shown for a few crystallographic directions. From the LDA bands, a loss function has been calculated. It is defined as

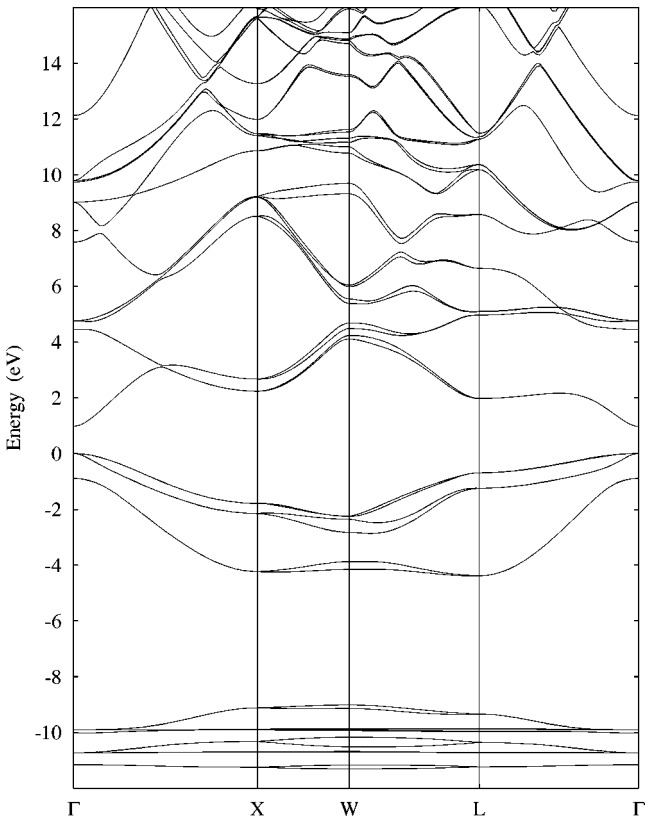

FIG. 1. LDA band structure of CdTe obtained with a semiempirical shift of Cd $4d$ states and including spin-orbit interaction.

$$W(\vec{q};\omega) = -\,\mathrm{Im}\,\epsilon^{-1}(\vec{q};\omega)_{\vec{G}=0,\vec{G}'=0}, \tag{1}$$

where ϵ^{-1} is the inverse, longitudinal dielectric matrix of the system. It can be represented by the following equation:

$$\epsilon^{-1} = 1 + v_c\chi^{(0)}[1-(v_c+f_{xc})\chi^{(0)}]^{-1}, \tag{2}$$

where all objects are matrices with respect to $\vec{G},\vec{G}'$, the reciprocal-lattice vectors. $\chi^{(0)}(\vec{q};\omega)_{\vec{G},\vec{G}'}$ is the density response of *noninteracting* Kohn-Sham electrons, $v_c = 4\pi/|\vec{q}+\vec{G}|^2\delta_{\vec{G},\vec{G}'}$ is the Coulomb interaction in the Fourier space and f_{xc} describes vertex corrections in the screening. Within the adiabatic LDA approximation,[23] f_{xc} is ω independent and is given by

$$f_{xc}(\vec{q},\omega)_{\vec{G},\vec{G}'} = f_{xc}(\vec{G}'-\vec{G}) = \int d^3r e^{i(\vec{G}'-\vec{G})\vec{r}}\frac{dV_{xc}(\vec{r})}{dn(\vec{r}')}\delta(\vec{r}-\vec{r}'), \tag{3}$$

where $V_{xc}(\vec{r})$ and $n(\vec{r}')$ are the self-consistent Kohn-Sham potential of the system and its electron density, respectively. The density response of noninteracting Kohn-Sham electrons $\chi^{(0)}$ has been calculated according to the well-known expression[23]

$$\chi^0(\vec{q},\omega)_{\vec{G},\vec{G}'}=\frac{2}{\Omega}\sum_{k}^{BZ}\sum_{n,n'}(f_{kn}-f_{k+qn'})\,\frac{\langle kn|e^{-i(q+G)r}|k+qn'\rangle\langle k+qn'|e^{i(q+G')r}|kn\rangle}{E_{kn}-E_{k+qn'}+\hbar\omega+i\delta}. \tag{4}$$

Convergence with respect to size of the matrix $(\vec{G},\vec{G}')$ (crystal *local-field* effects) and the uniform *k*-mesh sampling in the above expression has been very carefully checked. Our most accurate results have been obtained with the matrix size ranging between 83×83 and 90×90, depending on the momentum transfer and the *k* mesh of 10 976 points in the Brillouin zone (although much smaller meshes of 2048 and 864 *k* points give already convergent and acceptable results).

Most of our calculations have been performed without account of the spin-orbit splitting. However, in a few sample cases it has been checked that the inclusion of spin-orbit splitting does not lead to any significant changes in our results. This point will be briefly discussed below.

IV. RESULTS AND DISCUSSION

A. Experimental results

In Fig. 2, we present EELS measurements for the [111] and [110] directions at four different momentum transfers. The crystallographic directions were determined *in situ* using Bragg reflections in the electron diffraction pattern. Three dominant loss features *A*, *B*, and *C* are observed at energies of 11.9, 14.1, and 16.3 eV, respectively. The spectra are normalized to the intensity of peak *C* and shifted in their ordinate.

A comparison of the spectra for the [111] and [110] directions shows no significant differences indicating an isotropic dielectric function ϵ. While this is expected in the optical limit $(q=0)$ from symmetry arguments for a crystal with zinc-blende structure,[24] it is not necessarily the case for finite *q* values. The fact that even for a momentum transfer of 0.83 Å^{-1} no difference is observed for the two directions is rather surprising in view of the known anisotropy of nominally more free-electron semiconductors, e.g., Si.[25] We will discuss the reasons of such a behavior below.

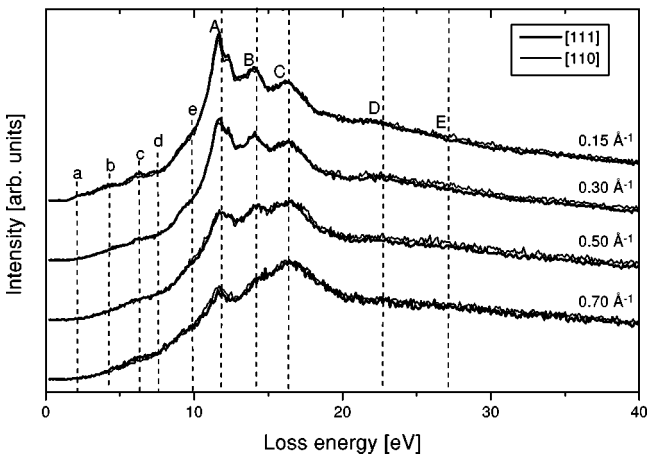

FIG. 2. CdTe EELS results for crystalline directions (111) and (110) at different momentum transfers *q*, collected at primary energy of 170 keV.

With increasing momentum transfer, significant changes in the shape of the spectra in Fig. 2 are observed. This is even more evident in Fig. 3(a) where the experimental spectra for the [111] direction are shown for more *q* values. Peak *A* is the dominant peak at low *q* values; it exhibits a doublet structure that is however not present for $q>0.3$ Å^{-1}. No dispersion is observed and its center of mass remains at 11.9 eV for all *q* vectors studied in our measurement. Peak *B* at 14.1 eV also displays no dispersion. The loss feature *C* at about 16.3 eV ($q=0.15$ Å^{-1}) shows a small positive dispersion with increasing *q*, up to about 16.8 eV ($q=0.83$ Å^{-1}). The intensities of peaks *A* and *B* decrease with increasing momentum transfer as compared to peak *C*.

In addition to the dominant losses *A*, *B*, and *C*, two broad spectral structures labeled *D* and *E* are observed at about 22.7 and 27 eV. These structures are more pronounced for small *q* transfers. At lower loss energies, four small features *a*, *b*, *c*, and *d* at 2.1, 4.2, 6.3, and 7.6 eV, respectively, and a shoulder *e* at 9.9 eV are observed for small momentum transfers (up to 0.3 Å^{-1}). The energies of these peaks agree well with the loss energies of 2.4, 4.4, 6.0, 7.6, and 10.4 eV observed in the REELS measurements using low primary energies.[9] These structures can be attributed to low-lying interband transitions or surface plasmons.

B. Comparison of measurements and calculations

The calculated loss spectra along the [111] direction are shown in Fig. 3(b) and compared to the experimental spectra from Fig. 3(a). Two sets of theoretical curves are presented, which correspond to different levels of approximation: the solid line gives the loss function obtained within the RPA approximation without inclusion of crystal local-field corrections, i.e., without considering the matrix form (in $\vec{G},\vec{G}'$ vectors) of the response functions (we call it a ''diagonal'' RPA approximation). The dashed line gives the loss function with the inclusion of both, crystal local fields and correlation effects within the time-dependent local density approximation (TDLDA). Due to the contribution of secondary losses at the high-energy side, it is difficult to determine an absolute scale for the experimental spectrum via, e.g., by normalizing with the *f*-sum rule. Therefore, there remains some arbitrariness in the scaling of experimental and theoretical intensities. In spite of this, it is remarkable how well both spectra agree. Except the doublet structure of peak *A*, all features observed in experiment are well reproduced by the calculations. Not only energetic positions of the calculated peaks agree rather well with the experiment, but also the relative intensities of peaks and various more subtle details of the measurements are reproduced. The fine structure of peak *A* is probably caused by the spin-orbit splitting of the Cd $4d$ states[26] and might be absent in the calculations due to the finite *k* mesh, which has to be used and which limits the resolution of the results. The fact that the agreement seems slightly better for the ''diagonal'' RPA calculation, than—what one would

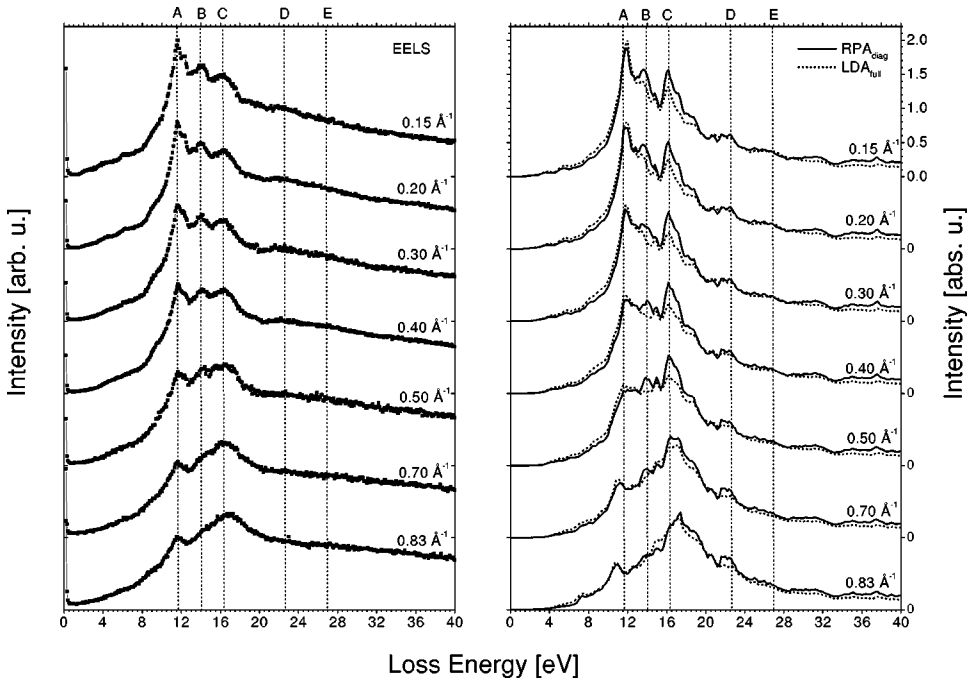

FIG. 3. Comparison of measured EELS spectra along the (111) direction [panel (a)] and the *ab initio* calculated loss function of CdTe [panel (b)]. Solid line in panel (b), RPA calculation without crystal local fields; dashed line, crystal local fields and many-body corrections (within TDLDA approximation) included.

expect—for the full-matrix LDA approximation, may have its rationale in the well known fact that the crystal local-fields and the many-body local-fields, i.e., the correlation effects, almost cancel each other. As it was shown in Ref. 27, both factors contribute to response functions with a similar strength; therefore the inclusion of only one of them can lead to the deterioration of the quality of the results. An example of such a situation in the density response of solid cesium has been discussed in Ref. 28. Our results from Fig. 3 seem to suggest that the TDLDA approximation underestimates the strength of the correlation effects in the screening for CdTe and that there should be a cancellation between the crystal and many-body local field effects.

The comparison of the experimental and theoretical spectra shows that the agreement in peak positions between experiment and theory is good, although not perfect. The best agreement is observed for structure *C*, which disperses positively in both theory and experiment by an amount of about 0.5 eV. The most evident difference is the presence of a small negative dispersion of the structure *A* in the theory and its absence in the experiment.

The tail of the spectrum for higher loss energies is almost structureless and has clearly a bigger amplitude in the experiment due to multiple scattering losses. Nevertheless, the two broader peaks in the experimental spectra at 22.7 and 27 eV (which we label *D* and *E*) are almost perfectly reproduced in the calculations, which, in addition, predict two less pronounced peaks at energies of 18.5 and 31.5 eV.

C. Discussion

The interpretation of EELS spectra is not a simple task and it is not always possible to unambiguously classify the experimentally observed structures as collective excitations or electron-hole interband transitions. In real materials, there exist in most cases interband transitions for all energies above the absorption threshold, also in the energy region of the onset of plasmons, which results in a coupled mode of collective and one-particle excitations. Nevertheless, the plasmon concept retains its validity as a damped collective excitation.[3] The situation gets complicated when significantly strong interband transitions appear in the plasmon energy region (which could be defined as the region where the real part of the dielectric function is close to zero). The presence of interband peaks leads to changes in the shape of $\mathrm{Re}(\epsilon)$, such that it becomes zero several times, or take a characteristic, ''saw-type'' shape. In effect, the loss function, $-\mathrm{Im}(1/\epsilon)=\epsilon_2/(\epsilon_1^2+\epsilon_2^2)$, where ϵ_1 and ϵ_2 are the real and imaginary parts of the dielectric function, respectively, can show a qualitatively new and unusual character, as compared with the cases of normal metals or semiconductors. For instance, the charge carrier plasmon energy and its dispersion are significantly reduced (enhanced) when a shallow core-level excitation comes to lie in the energetic neighborhood as it is observed for the late or post-transition metals.[29] As our calculations show, this is also the case for the dielectric function of CdTe and probably other II^B-VI compounds. In order to trace back the origin and character of various loss peaks in the spectra, we analyze the shape of the RPA dielectric function of CdTe for q vectors of 0.15 and 0.70 Å^{-1} in the [111] direction in Figs. 4 and 5, respectively. Panel (a) shows again the loss function, calculated without and with the spin-orbit splittings in the band structure (solid and dashed lines, respectively).[30] In panel (b) the relevant portions of the imaginary and real parts of the corresponding dielectric functions are depicted. In addition, in panel (c), $\mathrm{Im}(\epsilon)$ is decomposed into contributions originating from various occupied bands. In particular, the dotted line shows the contribution from Cd 4*d* states. The vertical dotted lines are drawn at the

theoretically obtained positions of the loss peaks *A*, *B*, and *C*. It is interesting to note, that the inclusion of spin-orbit interaction does not lead to any essential changes in the shape of the loss functions, as is concluded from Figs. 4(a) and 5(a). Therefore, in panels (b) and (c) of both figures we analyze the behavior of the dielectric function obtained without inclusion of this effect. It is seen that the peaks *A*, *B*, and *C* correspond either to a local minimum or to a turning point close to a minimum in $\mathrm{Im}(\epsilon)$ and a growing part of the ''sawlike'' portion of $\mathrm{Re}(\epsilon)$. The local peaks in $\mathrm{Im}(\epsilon)$, which are responsible for such a shape of the dielectric function, originate mainly from interband transitions with initial states in the Cd 4*d* bands [dotted line in panel (c)]. These peaks do not have the same energies as the loss peaks. In contrast, they are located in between the structures *A*, *B*, and *C*. This behavior seems to favor a ''collective'' nature of peaks *A*, *B*, and *C*, although the role played by the interband transitions from Cd 4*d* states is clear and the loss peaks have a pronounced contribution from these transitions. It is worth while to note that the usual condition for the appearance of a plasmon, namely $\mathrm{Re}(\epsilon)=0$, would be applicable only to the structure *A* [and even in this case not perfectly, because for larger *q* the loss peak *A* is slightly shifted with respect to the zero position of $\mathrm{Re}(\epsilon)$], whereas for the loss structures *B* and *C*, as well as for other, less pronounced peaks, this condition is not fulfilled. Nevertheless, it is just the structure *C*, which becomes most pronounced with growing *q*. For large *q* it would best correspond to a damped plasmon that one would obtain with the Cd 4*d* states frozen in the core. To quantify the last point, let us take the classical limit for the plasmon in CdTe as $E_p=(4\pi ne^2/m)^{1/2}=12.7$ eV and its dispersion coefficient within the RPA, given by $\alpha_{RPA}=\frac{3}{5}E_F/E_p=0.4$. Both numbers are calculated for the CdTe valence electron density of $n=0.0174$ a.u. As a result we obtain a free-electron plasmon energy of 16.8 eV for $q=0.70$ Å^{-1}.

The presence of a complex of a few loss peaks with a strong collective character renders the case of CdTe rather different from normal metals or semiconductors. We expect a similar situation for other compounds of the class II^B-VI, as well as for some of the class III-V. This observation is not exceptional, and the case of silver provides an example of a similar phenomenon, where the free-electron plasmon is split into one at 8 eV having a strong free-electron character, and one at 3.8 eV, for which a strong coupling to Ag 4*d* transitions takes place. Furthermore, the results presented here parallel the loss function of Zn where the shallow core excitations and the charge carrier plasmon strongly interact and the dispersion of the charge carrier plasmon is considerably reduced as a consequence of the spectral weight decrease of the shallow core excitations with increasing momentum transfer.[31]

In contrast to the peaks *A*, *B*, and *C*, the loss structures *D* and *E* have a clear character of an interband transition. As is seen in Figs. 4 and 5, these loss peaks have the same position as the interband peaks due to Cd 4*d* states in the $\mathrm{Im}(\epsilon)$ curves.

All above observations point out a very important role played by the Cd 4*d* states. Also the experimentally and computationally evidenced momentum isotropy of the loss function (see Fig. 2) seems to originate from the same reason. The very flat, almost dispersionless Cd 4*d* bands contribute to the $\mathrm{Im}(\epsilon)$ function with a very small $\vec{q}$ dependence, in both, modulus and direction. Since the influence of these bands on the shape of the loss function is so strong, it results in the isotropy of the loss properties of CdTe.

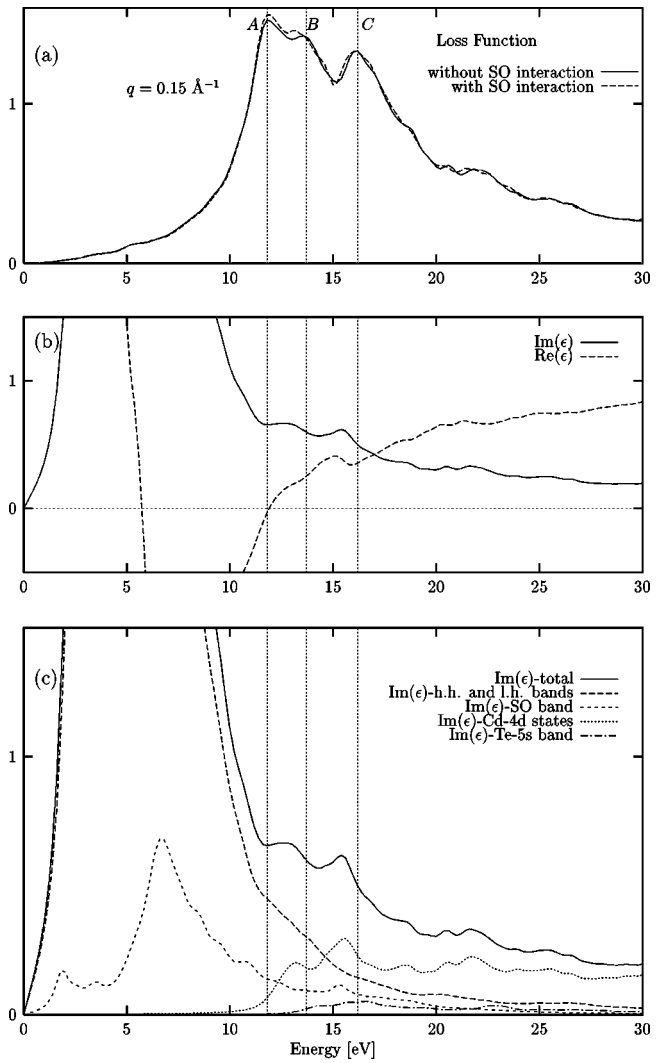

FIG. 4. Panel (a): loss function of CdTe with (dashed line) and without (solid line) spin-orbit splittings in the band structure for $q=0.15$ Å^{-1} in the (111) direction. Panel (b): $\mathrm{Im}(\epsilon)$ (solid line) and $\mathrm{Re}(\epsilon)$ (dashed line) for the same *q*-vector as in (a). Panel (c): $\mathrm{Im}(\epsilon)$ decomposed into contributions coming from various occupied bands; heavy-holes (h.h.) and light-holes (l.h.) upper bands (long-dashed line), spin-orbit (SO) splitted band (short-dashed line), Cd 4*d* states (dotted line), Te 5*s* band, i.e., the lowest occupied valence band (dashed-dotted line).

An interesting difference between the calculated spectra and experiment is the dispersion of the loss structure *A*. While this feature does not seem to disperse in the experimental spectra, it shows a *negative* dispersion of about 0.8 eV between $q=0.15$ and $q=0.83$ Å^{-1} in the calculations. This negative dispersion is observed for all versions of calculations, i.e., with and without spin-orbit splitting, with and without the crystal local-field effects, as well as within the RPA and the TDLDA approximations. The careful analysis of this behavior reveals that with a growing *q* vector a small peak at 12.2 eV in the $\mathrm{Im}(\epsilon)$ function appears, which is

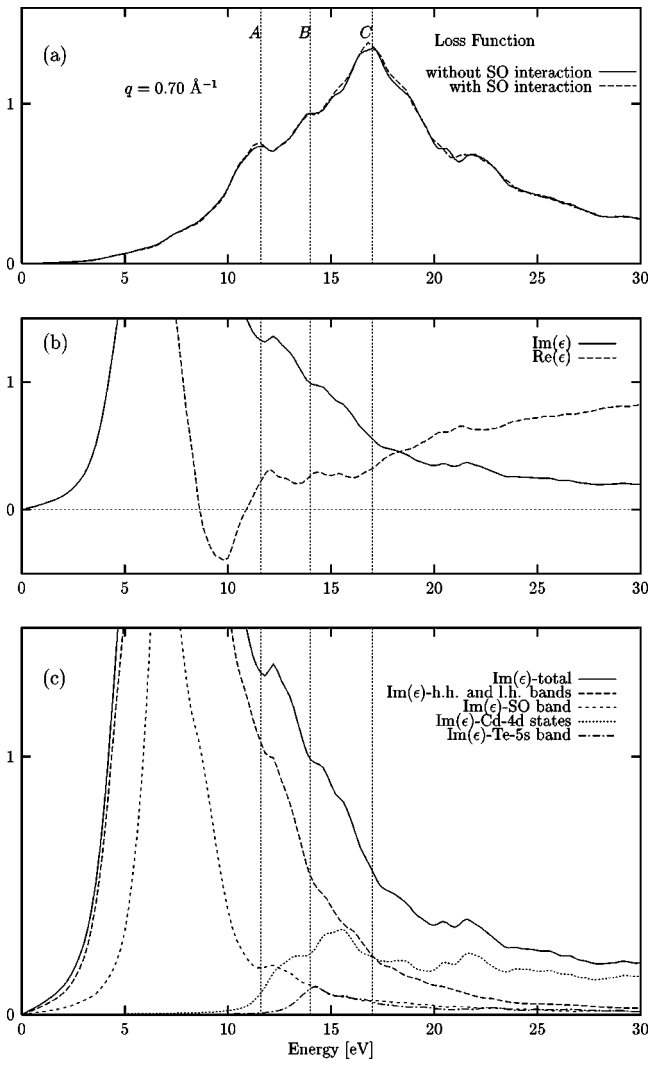

FIG. 5. Same as Fig. 4 for $q=0.70$ Å^{-1} in the (111) direction.

mostly due to transitions from the spin-split band (the SO band). This peak, supported by a growing tail of the main electron-hole peak in the Im(ϵ) function, which in analogy with the metal case could be called a ''Drude peak,'' dominates the peak at 13 eV due to Cd 4*d* states, which in the total Im(ϵ) curve for $q=0.70$ Å^{-1} remain only as a shoulder. This kind of behavior seems not to occur in experiment. There could be several reasons for this discrepancy: One of them could be an energy shift of the interband peak at 12.2 eV in calculations, due to self-energy corrections on the higher conduction bands. Another reason could be a well-known fact that the correlation effects in screening (e.g., the excitonic effects) tend to increase the spectral weight of Im(ϵ) for small energies at the cost of spectral weight at higher energies, what is necessary for the fulfillment of sum rules. The importance of such correlation effects should in general grow with a growing *q*. Therefore, the descending part of the Drude peak could be in reality less pronounced than in the RPA (and TDLDA) calculation and possibly the peak at 13 eV would still dominate. These are hypotheses that are rather difficult to check computationally, although first attempts to include such effects in *ab initio* calculations for real materials have recently appeared.[32–35]

V. SUMMARY

We have presented results of the high-resolution electron energy-loss measurements of films of CdTe single crystals. The loss function in the [111] and [110] crystallographic directions for momentum transfers ranging between 0.07 and 0.83 Å^{-1} was experimentally investigated. Our results show a rather unusual shape of the loss function composed of a complex of a few intense and well-resolved structures of comparable strength occupying a rather narrow energy region of 5 eV around the classical plasmon energy. These structures show no or small dispersion and are isotropic with respect to the direction of the momentum transfer. A detailed analysis of the experimental spectra using *ab initio* calculations of the CdTe dielectric function points out the very important role played by the semicore Cd 4*d* states in the loss properties of CdTe. Our results indicate that a similar behavior is to be expected in other materials possessing localized semicore states, which give rise to interband transitions in the energy range of the plasmon due to the valence electrons. This concerns in particular other semiconductors from the class II^B-VI.

ACKNOWLEDGMENTS

This work was supported by the Deutsche Forschungsgemeinschaft through SFB 410. We thank Dr. V. Wagner for discussing the optical data with us and Professor G. Schütz for her assistance in sample preparation. Especially, we thank Th. Gerhardt for performing x-ray diffraction measurements. The calculations have been done at the Leibnitz Rechenzentrum in Munich.

[1] H. Raether, *Excitation of Plasmons and Interband Transitions by Electrons*, Springer Tracts in Modern Physics Vol. 88 (Springer-Verlag, Berlin, 1980).
[2] J. D. Jackson, *Classical Electrodynamics* (Wiley, New York, 1962).
[3] K. Sturm, Adv. Phys. **31**, 1 (1982).
[4] J. Fink, Adv. Electron. Electron Phys. **75**, 121 (1989).
[5] A. Ebina, K. Asano, Y. Suda, and T. Takahashi, J. Vac. Sci. Technol. **17**, 1074 (1980).
[6] J. Gordon, P. Morgen, H. Shechter, and M. Folman, Phys. Rev. B **52**, 1852 (1995).
[7] A. Dittmar-Wituski, M. Naparty, and J. Skonieczny, Surf. Sci. **213**, 254 (1989).
[8] R. L. Hengehold and F. L. Pedrotti, Phys. Rev. B **6**, 2262 (1972).
[9] H. Dröge, A. Fleszar, and H.-P. Steinrück, J. Cryst. Growth **184/185**, 208 (1998).
[10] B. Gauthé, Phys. Rev. **114**, 1265 (1959).
[11] T. Tomoda and M. Mannami, J. Phys. Soc. Jpn. **27**, 1204 (1969).
[12] C. J. Rossouw, S. R. Glanvill, and G. N. Plain, in *Microscopy of Semiconducting Materials 1989*, Proceedings of the Royal Microscopical Society Conference, edited by A. G. Cullis and Y. L. Hutchinson (Institute of Physics, Bristol, 1989), p. 229.

[13] J. L. Freeouf, Phys. Rev. B **7**, 3810 (1972).
[14] D. E. Aspnes and H. Arwin, J. Vac. Sci. Technol. A **2**, 1309 (1984).
[15] T. Kimura and S. Adachi, J. Phys. Soc. Jpn. **32**, 2740 (1993).
[16] A. D. Brothers and J. B. Brungardt, Phys. Status Solidi B **99**, 291 (1980).
[17] N. Boudet, J. Eymery, G. Renaud, J. L. Rouvière, J. Y. Veuillen, D. Brun, and B. Daudin, Surf. Sci. **327**, L515 (1995).
[18] A. Fleszar and W. Hanke, Phys. Rev. B **56**, 12 285 (1997).
[19] T. Gerhardt, H. Dröge, F. Goschenhofer, W. Faschinger, and H.-P. Steinrück (unpublished).
[20] G. B. Bachelet, D. R. Hamann, and M. Schlüter, Phys. Rev. B **26**, 4199 (1982).
[21] We have used the parametrization by P. Perdew and A. Zunger, Phys. Rev. B **23**, 5048 (1981); of the results of D. M. Ceperley and B. I. Alder, Phys. Rev. Lett. **45**, 566 (1980).
[22] W. Kohn and L. J. Sham, Phys. Rev. **140**, A1133 (1965).
[23] E. K. U. Gross and W. Kohn, Adv. Quantum Chem. **21**, 255 (1990).
[24] P. Y. Yu and M. Cardona, *Fundamentals of Semiconductors* (Springer, Berlin, 1996), Chap. 6.
[25] W. Schülke, J. R. Schmitz, H. Schulte-Schrepping, and A. Kaprolat, Phys. Rev. B **52**, 11 721 (1995).
[26] A. Wall, Y. Gao, A. Raisanen, A. Franciosi, and J. R. Chelikowsky, Phys. Rev. B **43**, 4988 (1991).
[27] W. Hanke and L. J. Sham, Phys. Rev. B **21**, 4656 (1980).
[28] A. Fleszar, R. Stumpf, and A. G. Eguiluz, Phys. Rev. B **55**, 2068 (1997).
[29] M. Knupfer, K. Widder, M. Sing, O. Knauff, and J. Fink, Eur. Phys. J. B **6**, 323 (1998).
[30] We use a small, but finite value of the parameter δ in Eq. (4), which is a convergence parameter when the sum over continuous set of k vectors is approximated by a discrete sum. In our most precise calculations from Fig. 3(b) the value of δ was 0.1 eV, while in Figs. 4 and 5 its value was 0.4 eV, which results in more smooth curves.
[31] K. Widder, M. Knupfer, O. Knauff, and J. Fink, Phys. Rev. B **56**, 10 154 (1997).
[32] F. Bechstedt, K. Tenelsen, B. Adolph, and R. Del Sole, Phys. Rev. Lett. **78**, 1528 (1997); V. I. Gavrilenko and F. Bechstedt, Phys. Rev. B **55**, 4343 (1997).
[33] S. Albrecht, L. Reining, R. Del Sole, and G. Onida, Phys. Rev. Lett. **80**, 4510 (1998).
[34] M. Rohlfing and S. G. Louie, Phys. Rev. Lett. **80**, 3320 (1998).
[35] E. L. Shirley, Phys. Rev. Lett. **80**, 794 (1998); L. X. Benedict, E. L. Shirley, and R. B. Bohn, Phys. Rev. B **57**, R9385 (1998); Phys. Rev. Lett. **80**, 4514 (1998).